Variable recruitment of parallel elastic elements: Series-Parallel Elastic Actuators (SPEA) with dephased mutilated gears

Glenn Mathijssen *Student member, IEEE,* Dirk Lefeber *Member, IEEE,* and Bram Vanderborght, *Member, IEEE*

***Abstract*—The development and control of Variable Stiffness Actuators (VSAs) led to the capability of embodying physical principles of safety and energy-efficiency compared to traditional stiff servomotors. However, the output torque range and efficiency of servomotors and VSAs are still insufficient which hinders the development of machines with performances comparable to a human. We have developed a novel compliant actuation concept, Series-Parallel Elastic Actuation (SPEA), that addresses these problems. The novelty being the variable recruitment of parallel elastic elements and adaptive load cancellation. In this paper we propose the use of multiple dephased mutilated gears with locking ring and plate, as intermittent mechanisms, linked in parallel to the motor. As a result, the motor torque requirements can be lowered, as such the motor can be downscaled and the efficiency can be drastically increased. After an abstract description of the SPEA concept and an outline of the biological basis, we present the first unidirectional SPEA Proof of Concept (PoC) set-up. Experiments on this PoC set-up endorse the feasibility of the SPEA concept. The results match the modeled trend of a lowered motor torque and increased energy efficiency.**

***Index Terms*—Compliant actuation, new actuators for robotics, energy efficient actuators, high torque output, intermittent mechanism and SPEA**

I. Introduction and problem analysis

Actuators are key components for moving and controlling a mechanism or system. Servomotors are generally used for industrial robots. As they make the joint's mechanical impedance very high, they are ideal for precise position tracking with a high bandwidth. Servomotors typically consist of an electric motor connected to a gearbox to reduce the rotation speed and to increase the torque. The dynamics of an actuator influences the global control of the robotic system through its mass, inertia, stiffness, etc. However, servomotors have a bad trade-off between adaptability and performances, i.e. they cannot simultaneously satisfy safety and, trajectory and energy efficiency performances if output impedance is high.

A major step in this aim was the introduction of an actuator having an elastic element in series with the motor. Such an actuator is commonly named a Series Elastic Actuator (SEA), as introduced by Pratt about 2 decades ago [1]. The compliance enabled to decouple the inertia from one link to the other over the spring, which is beneficial for safety and shock-absorbance [2]. Furthermore, the spring is an energy buffer, reducing the power rating of the motor by making it work over a longer period of time [3] but with less power, or by storing and releasing energy.

The authors are with the research group Robotics & Multibody Mechanics at the Vrije Universiteit Brussel, Pleinlaan 2, 1050 Brussel, Belgium. (e-mail: glenn.mathijssen@vub.ac.be and phone: +32-2-6292862)

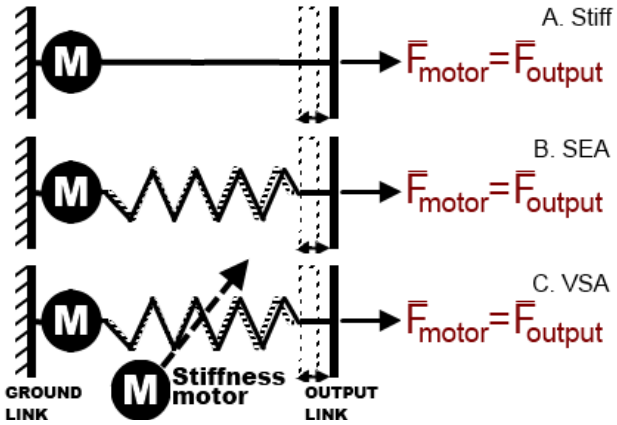

Fig. 1. Actuator schemes to illustrate that $F_{motor} \cong F_{output}$ for a stiff actuator, a SEA and a VSA.

Many designs ensued with a mechanism with an extra motor enabling to change the stiffness of the spring, referred to as Variable Stiffness Actuators (VSAs)[1]. VSAs allow to exploit and adapt the natural dynamics of a system by controlling the stiffness [7]. Examples are: pneumatic artificial muscles [7], [8], MACCEPA [9], AMASC [10], AwAS [11], AwAS-II [12], Floating Spring Joint [13] and many others described in literature. An overview with classification of these actuators is given in [14].

Numerous research projects emerged where intrinsic joint elasticity is an essential design parameter. More recently, SEAs found their way to the market too with for example Mekabot [15] and Baxter from RethinkRobotics [16]. The advances in VSA technology is paving the way towards new application fields, such as industrial co-workers, household robots, advanced prostheses, rehabilitation devices and other autonomous robots [17].

Despite of the advances in both stiff and bio-inspired compliant actuation schemes, the current actuation technology is often still inadequate for (mostly novel) applications with versatile output requirements and required autonomy (e.g. exoskeletons, humanoids, prostheses, manipulators, etc.). The

[1]Currently, these actuators are also referred to in literature as Variable Impedance Actuators or VIAs (a more general name for active impedance by control, inherent compliance and damping actuators [4], inertial and a combination of them) [5], [6].

main problem is that actuators (servomotor, gearbox and possibly springs) with a wide output profile (torque, velocity and power) are generally bulky, heavy and inefficient [6] [18]. For example, a powered prosthesis for fast walking, running or agile locomotion does not yet exist and in more functional exoskeletons (such as the Raytheon XOS2), the hydraulic power generation is anchored to the reference base and transported by tubes to the joints. Other examples are the biped Atlas and the horse-robot LS3 which have a mechanical efficiency of 1% compared to a human or horse respectively, limiting the use of the robots to only one hour [19].

On the contrary, the average specific power density of a mammalian skeletal muscle (0.05 W/g) is an order of magnitude lower compared to electric motors (0.5 W/g) [20]. The maximum efficiency of an electric motor (>80%) is also higher than that of a muscle (<40%). Despite this higher power density and motor efficiency, mechatronic systems powered by electric motors are not yet able to offer the agility, dexterity and versatility of biological muscles. Therefore, we believe the way transmissions and springs are used needs drastic innovation.

An abstract model of a servomotor is a motor connected in series with a gearbox and the load. Likewise, all SEA set-ups can be schematized by a motor connected in series with a gearbox, a spring (torsional for rotational joint and linear for a prismatic joint) and the load. The most basic scheme of a VSA is that of a SEA with an extra motor added to change the stiffness as indicated in Fig. 1.C. The main disadvantage of these serial designs (servomotor, SEA and VSA) is that all the torque generated by the actuator, also stresses the motor that controls the equilibrium position. As a result, a SEA or VSA can only lower the required motor power profile by storing and releasing energy in the spring and lowering the motor speed, but not the motor torque or force. The antagonistic setups are a subset of the VSAs. The torques and energy consumption on the 2 motors of the antagonistic set-up are higher compared to the serial set-up [21], later confirmed in [22]. Reason is that the torque on the biggest loaded actuator is the sum of the torque required at the output plus the torque needed to generate the desired stiffness.

One method that modifies the range of external forces or torques that can be applied to a mechanical system is the use of a spring in parallel to a servomotor. This concept is referred to in literature as Parallel Elastic Actuation (PEA) and is for example described by [23]. The idea is that the parallel spring generates most of the nominal torque required to follow a given trajectory and the actuator only provides the difference. Statically balanced mechanisms for gravity compensation, keeping the potential energy constant in any configuration, often deploy a parallel spring [24], [25]. Deploying an elastic element in parallel with a servomotor, however, leads to a stiff output, canceling the above mentioned advantages of a compliant actuator. To overcome this, an additional elastic element in series with the motor is required. Another disadvantage of PEAs is that they limit movement dexterity. As the parallel spring is always engaged and fixed in the design phase, these actuators tend to recoil the stored energy and induce joint motions that counter desired ones in acyclic movements. For the specific case of a powered ankle-foot prosthesis, this can be resolved by installing a uni-directional spring in parallel with a force controllable SEA [26]. For more general applications, designs emerged with a clutching mechanism connected to the parallel spring, like the compact version of the Clutched Parallel Elastic Actuator (CPEA) for example [27]. These designs however consume power when engaged and become relatively large when the torque range increases.

The novelty of this paper is that we propose a series-parallel arrangement with variable recruitment of multiple parallel elastic elements for compliant joint actuation and adaptive load cancellation. We call this novel actuation concept: Series-Parallel Elastic Actuation or SPEA and we propose the use of multiple dephased intermittent mechanisms, with internal locking, linked in parallel to the motor. This paper is organized as follows: after the SPEA concept is presented in section II, the biological inspiration for the SPEA concept is elaborated in section III. The Proof of Concept (PoC) set-up is presented in section IV, followed by section V discussing the experimental results of the PoC set-up. We conclude with a discussion of the potential of the SPEA concept and possible future work.

II. Concept

A. General description of the SPEA concept

The SPEA presented in this work consists of a bundle of parallel compliant elements (typically springs), for which every spring can be tensioned in succession to increase the output force or torque of the SPEA (in this section we will use force schematics for simplicity). As shown in Fig. 2, each parallel spring is connected with one side to the output link. The other side of each spring is connected to the output of one of the parallel dephased intermittent mechanisms. This general SPEA concept is theoretically introduced in [18]. An intermittent mechanism converts a continuous (rotational) input to 2 consecutive phases [28]:

1) *Motion phase:* the output is actuated by the input;
2) *Dwell phase:* the output is blocked while the input rotates freely.

The idea now is to place n intermittent mechanisms in parallel (one for each of the n parallel springs), dephase each input relative to its predecessor and fix each input of the intermittent mechanisms to the same shaft that is connected to the output of a stiff servomotor. The output of each intermittent mechanism is then connected to one of the n parallel springs. As such, the total mechanism enables to tension and lock the n parallel springs in the SPEA successively. This is indicated by the servomotor in Fig. 2 (solid black circular motor symbol) which can shift position (indicated by the shaded motor symbols). A single spring of the SPEA can be in three phases as shown in Fig. 2:

1) *The unpretensioned phase:* the intermittent mechanism is in the dwell phase, the spring is at its rest length and fixed to the ground link and the output link. All forces that are exerted will not pass through the motor since it is not present in the force path (shaded motor);

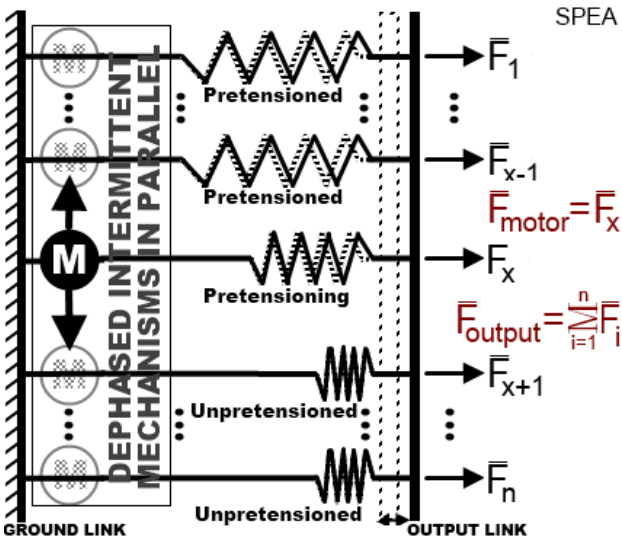

Fig. 2. Principle scheme of a SPEA with dephased intermittent mechanisms in parallel. In comparison to the actuators in Fig. 1, F_{motor} is only a fraction of F_{output} for a SPEA.

2) *The pretensioned phase:* the intermittent mechanism is in the dwell phase, the spring is fully extended and fixed to the ground link and the output link. All forces that are exerted will not pass through the motor since it is not present in the force path (shaded motor);
3) *The pretensioning phase:* the intermittent mechanism is in the motion phase, the motor controls the length of the spring and brings it from unpretensioned phase to pretensioned phase or back. The forces that are exerted will pass through the motor since it is present in the force path (solid black motor).

Only the forces that are exerted on the spring in the pretensioning phase will go through the motor. Since most of the springs are in the unpretensioned or in the pretensioned phase and only one or a few are in the pretensioning phase, only a fraction of the total force exerted on the output link will be felt by the motor as indicated by the force vectors in Fig. 2. Through this virtue, the SPEA concept enables to reduce the force or torque requirements of the motor and to increase the efficiency.

B. Realization of the SPEA concept

An intermittent mechanism with internal locking (during the dwell phase) can be achieved with different mechanical principles [28] [29]. Most designs are based on ratchets or cam mechanisms (e.g. the Geneva drive). The preferred designs should not require an extra motor and should not induce large friction levels or shocks. This paper proposes the use of mutilated gears for the first SPEA PoC, which is described in section IV. The basic concept of mutilated gears consists of removing a number of teeth of the driver of a pair of (spur) gears. As a result, the continuously turning driver only drives the driven output when the teeth interact, which results in an intermittent motion. The placing of a locking ring and plate ensures that the driven output is locked during the dwell phase. Pairs of mutilated gears in dwell phase, the transition from dwell to motion phase, and in motion phase are presented in Fig. 3. The different components of the mutilated gears are indicated as well. Mutilated gears offer design freedom regarding the motion curves since the length of the dwell phase depends on the number of teeth removed. Furthermore, multiple dwell and motion phases can be easily obtained by alternating sections of the driver gear where teeth are removed and where teeth are not removed, and the length of each dwell and motion phase can be chosen individually as well. Finally, since mutilated gears are adapted normal gears, the gear ratio can still be chosen. The main disadvantage is the impact produced at the start of every motion phase. An important issue regarding the use of mutilated gears in the SPEA, is the blocking of the mechanisms at the transition from the dwell phase to the motion phase, when the output load (torque in this case) is in the same (rotational) direction as the input motion. This is indicated in Fig. 3 by means of the lower light blue tooth that should follow the arrow in order to avoid blocking of the mechanism. Due to the output load (indicated by the arrow and explanation mark), however, the two light blue teeth interact and the mechanism blocks. In other words, the intermittent mechanism skips a tooth. This problem, of blocking when the driven output is under load, is common to most intermittent mechanisms. To bypass this problem, the spring is connected to a lever arm, which is fixed to the driven output. The dephased mutilated gear mechanisms tension each spring successively from the singular position of no torque at the lever arm at $0°$, to the next singular position at $180°$. This is indicated in Fig. 4 where the first two springs are pretensioned and thus ϕ_1 and ϕ_2 are equal to $180°$. As a result, the transition from dwell phase to motion phase is without any load on the output due to the singular position, and the mechanism does not block. For a perfect transition, the driving shaft of the mutilated gears is notched more than half. As such, a small torque opposite to the direction of the driver input ensures the mechanism does not block. A second advantage of locking in a singular position of no torque at the lever arm, is the reduction of friction levels in the dwell phase between the locking ring and plate.

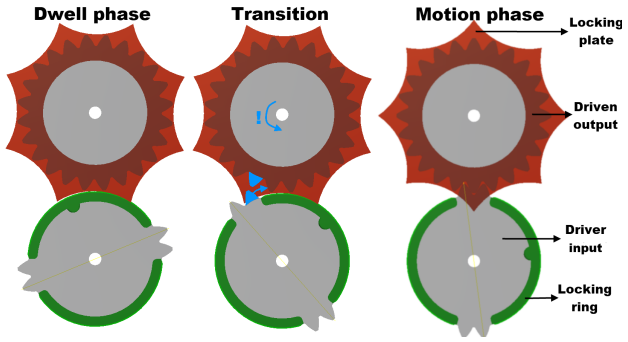

Fig. 3. Schemes of a pair of mutilated gears in the dwell, transition and motion phase. The potential blocking under load is illustrated by the two light blue teeth in the transition phase.

III. Biological inspiration

The development of variable stiffness actuators [17] and extend impedance control as humans [30] is strongly inspired

by the working principle of skeletal muscles, where the elasticity plays a major role during motion [31]. The use of elastic elements is presented in the systems engineering perspective of a purely mechanical muscle model in, for example, Hills macroscopic three element elastic muscle model. It consists of a Contractile Element (CE), a Series Elastic Element (SE) and a Parallel Elastic Element (PE) [32]. The similarity between these three elements and the current state of the art of compliant actuation concepts is clear. The CE and SE can be linked respectively to the stiff motor and serial spring of current SEAs and VSAs. The more recent designs with a parallel spring, the PEAs, can be linked to the PE of Hill's three element model. A combination of all three elements can be found for example in the powered ankle-foot prosthesis of Hugh Herr [26].

We found inspiration for our SPEA concept beyond Hill's macroscopic three element model, in the biological muscle, which consists of a large set of parallel and series motor units in connection with neurons. The force produced by a single motor unit is partly determined by the number of muscle fibers in the unit. A muscle can be progressively activated by successive motor unit recruitment [33]. This means that by changing the number and size of motor units triggered, a muscle can change its strength of contraction. In order to lift a light object only a small number of motor units are recruited, whilst more and more motor units are recruited to lift a heavier object. The difference with our novel SPEA concept is that not all springs in the SPEA need their own motor unit (generally an electric motor). Instead, a single motor with an intermittent mechanism controls the engagement of several parallel springs. These biological foundings provide a logic amenability for the study of variable recruitment of parallel compliant elements for reduced motor torque and energy requirements.

IV. Proof of Concept

This section describes the PoC built in order to validate the feasibility of the SPEA concept with intermittent mechanism, and the reduction in motor torque and energy requirements as a function of increased number of parallel springs. A scheme of the PoC is provided in Fig. 4 and an overview picture in Fig. 5.A.

A. PoC mechanical set-up

The PoC consists of 4 springs. This is enough to show the working principle, while more springs would further decrease the maximum motor torque. Each spring is connected by means of wires to one of the lever arms on the input side, and to one of the drums on the output side. Since the wires are wrapped around one side of the drums, the output torque is unidirectional. The driver of each parallel mutilated gear mechanism is fixed to the input shaft, which is connected to a servomotor. The drivers of the mutilated gear mechanisms are mutually dephased and each have one dwell phase and one motion phase. The driven outputs of the mutilated gear mechanisms are connected to the lever arms and rotate freely around the lever arm shaft. A locking plate and locking ring are installed to provide locking in the dwell phase. One can easily see that these will be subject to friction. Reducing friction between the locking ring and locking plate of the mutilated gear mechanisms is accomplished by locking the springs, in both unpretensioned and pretensioned phase, in a singular position of no torque at the lever arm. This means that each of the lever arms should be turned over 180°. Since the PoC consists of 4 lever arms that each should turn over 180°, the gear ratio of the mutilated gear mechanisms should be $\epsilon = \frac{1}{2}$ so that the driver shaft of the mutilated gear mechanism turns through 360° in order to tension all 4 springs.

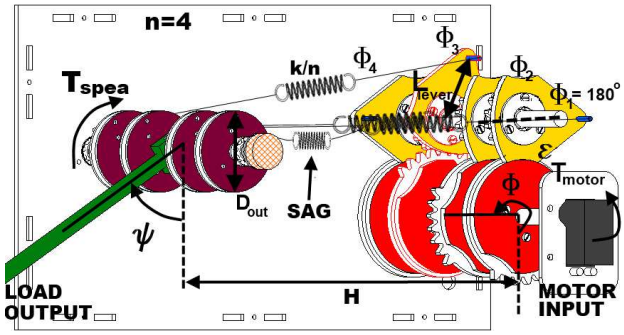

Fig. 4. All relevant SPEA parameters indicated on a scheme of the PoC.

The springs in the PoC are turned to the pretensioned phase one by one in order to increase the generated torque T_{SPEA}. In Fig. 4, the most important angles, torques and parameters of the PoC are shown. It is important to note that in this agonistic set-up the springs in the unpretensioned phase clearly sag. The unpretensioned springs are at rest length at $\phi_i = 0$. When the output angle $\psi \neq 0$, the unpretensioned springs sag. As a result, the stiffness regarding the output is smaller than $n\frac{k}{n} = k$. The effect of sagging springs will be implemented in the theoretical model here underneath.

B. PoC theoretical model

In this section all equations needed to calculate the motor torque T_{motor} and motor velocity ω_{motor} w.r.t. a certain required torque T_{req} and angular velocity ω_{req} profile at the output will be derived. The following list contains all relevant parameters of the PoC as indicated in Fig. 4:

- n = number of springs in parallel;
- ϕ = motor input angle;
- ψ = output angle;
- ϕ_i = angle of lever arm i;
- k/n = spring constant of one spring in a SPEA set-up with n springs;
- L_{lever} = input lever arm length;
- D_{out} = output drum diameter;
- H = horizontal distance between driver shaft and lever arm shaft;
- $\epsilon = \frac{1}{2}$;
- T_{motor} = motor torque;
- ω_{motor} = angular motor velocity;
- T_{SPEA} = torque applied by the SPEA.

If the angle on the motor side is ϕ, then all input drums are positioned at specific angles ϕ_1 *to* ϕ_n. The angular position

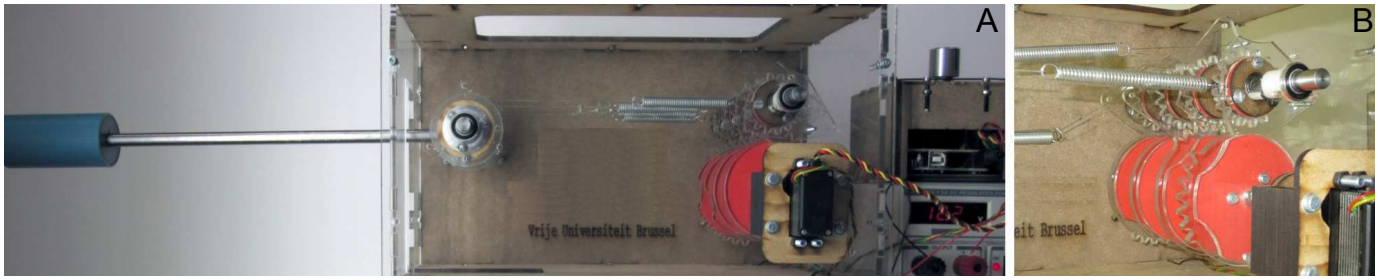

Fig. 5. Overview picture of the SPEA PoC (left) and a close-up of the mutilated gears (right).

of the input drum that is actuated by the motor at a certain moment, ϕ_{Actual}, depends on the motor angle ϕ and on the design of the mutilated gears. The angular position of any input drum can be found by ϕ_i. Both expressions can be found in (1) and (2). Abs(x) stands for the absolute value of x. Furthermore, $\frac{x+abs(x)}{2}$ returns x for $x > 0$ and returns 0 for $x \leq 0$. Variations of $\frac{x+abs(x)}{2}$ are used in (1) and (2) to equal specific terms to 0, once they are bigger or smaller than a certain limit value. Fix(x) rounds x to the nearest integer towards zero.

$$\begin{aligned}\phi_{actual}(\phi) =& \frac{-1}{\epsilon}\left(\phi - fix\left(\frac{\phi}{\frac{2\ \pi}{n}}\right)\frac{2\ \pi}{n}\right.\\ &\left.+fix\left(\frac{fix\left(\frac{\phi}{\frac{2\ \pi}{n}}\right)}{n}\right)\frac{2\ \pi}{n}\right)\end{aligned} \tag{1}$$

$$\begin{aligned}\phi_i(\phi) =& \left(\frac{\phi-(i-1)\frac{2\pi}{n}+abs\left(\phi-(i-1)\frac{2\pi}{n}\right)}{2}+\frac{2\pi}{n}\right)\frac{1}{2}\\ &-abs\left(\frac{\phi-(i-1)\frac{2\pi}{n}+abs\left(\phi-(i-1)\frac{2\pi}{n}\right)}{2}-\frac{2\pi}{n}\right)\frac{1}{2}\end{aligned} \tag{2}$$

As ϕ_{actual} and ϕ_i were defined for the angle ϕ, Ext_{actual} and Ext_i are defined for the spring extensions in (3) and (4).

$$\begin{aligned}&Ext_{actual}(\phi,\psi_{req}) =\\ &\left(L\left(-\epsilon\phi_{actual}\left(\phi\right)\right)+L_{lever}-H+\frac{\psi_{req}D_{out}}{2}\right)\frac{1}{2}\\ &-abs\left(L\left(-\epsilon\phi_{actual}\left(\phi\right)\right)+L_{lever}-H+\frac{\psi_{req}D_{out}}{2}\right)\frac{1}{2}\end{aligned} \tag{3}$$

$$\begin{aligned}&Ext_i(\phi,\psi_{req}) =\\ &\left(\left(L\left(\phi_i(\phi,i)\right)+L_{lever}-H+\frac{\psi_{req}\,D_{out}}{2}\right)\right.\\ &\left.-abs\left(L\left(\phi_i(\phi,i)\right)+L_{lever}-H+\frac{\psi_{req}\,D_{out}}{2}\right)\right)\frac{1}{2}\end{aligned} \tag{4}$$

All the above mentioned parameters will now be used to calculate the motor angular position ϕ_{motor}, the motor angular velocity ω_{motor} and the motor torque T_{motor} as a function of the desired output torque T_{req} at ψ_{req}. The motor angular position ϕ_{motor} can be found by iteration. ϕ_{motor} is equal to the value ϕ that matches (5):

$$T_{req} = \sum_{i=1}^{n} -\frac{k}{n}\frac{D_{out}}{2}\,Ext_i(\phi,\psi_{req}) \tag{5}$$

Derivation of ϕ_{motor} leads to ω_{motor}. The motor torque T_{motor} can now be found by means of (6) here underneath and the knowledge of ϕ_{motor} from the iteration of (5):

$$\begin{aligned}T_{motor} =& \frac{1}{\epsilon}\frac{k}{n}\\ &\sin\left(\beta(-\epsilon\,\phi_{actual}(\phi))\right)L_{lever}\,Ext_{actual}(\phi,\psi_{req})\end{aligned} \tag{6}$$

C. PoC realization

An overview picture of the PoC and a close-up of the mutilated gears, designed and built for this paper is presented in Fig. 5.B and a sketch in Fig. 6.C. Apart from some machined aluminum connectors and the shafts, all parts are in MDF (Medium-density fiberboard) and Plexi, and cut by laser. This allows rapid prototyping and significantly reduces the production costs. By leaving enough space between the springs and using Plexi sides, a set-up where the working principle is clearly visible is obtained. Moreover, the configuration can be altered for making a setup with 2 parallel springs or a single spring. Dimensions can be reduced for implementation in different applications. An Arduino board with custom-design PCB is used to control the device and preform the measurements. A current sensor (ACS712 fully integrated, Hall effect-based linear current sensor IC) is installed over the DC motor poles as well as a voltmeter, to measure the electric motor power. The measured current is used to calculate the motor torque. The gravitational output torque can be calculated indirectly since the output angle ψ is known by measurement, as well as the mass connected to the output arm and the length of the output arm. The servomotor that drives the PoC SPEA with 4 springs is a HITEC HS-5955TG coreless digital servomotor with a 4-stage titanium gearbox. The servomotor is modified to enable continuous rotation. The documented parameters are: gear ratio 347:1, R = 1.4 Ω, $I_{stall} = 4.2\,A$ and $T_{stall} = 2.35\,Nm$. Finding the other motor parameters for a Hitec servomotor is difficult. That is why for the following parameters we made estimations via electric motors of comparable size and power: $\nu = 12\,10^{-7}\,\frac{Nm}{\frac{rad}{sec}}$, $M = 4.4\,10^{-7}\,Kgm^2$ and a gearbox efficiency of 50%. Each spring in the PoC SPEA with 4 springs has a stiffness of $350\frac{N}{m}$ and rest length $0.05\,m$.

In order to compare the experimental results of the SPEA PoC with 4 springs, the PoC is converted to 3 other set-ups. A stiff set-up which is driven by the same HITEC servomotor as the PoC with 4 springs (a scheme in Fig. 6.A). An SPEA set-up with only 2 springs of which the stiffness is doubled to $700\frac{N}{m}$ (practically realized by combining 2 springs of $350\frac{N}{m}$ in parallel). An SEA set-up with spring stiffness is quadrupled to $1400\frac{N}{m}$ (practically realized by combining 4 springs of $350\frac{N}{m}$ in parallel). The servomotor is again the same HITEC. The experimental results will be discussed in section V.

D. DC motor model

At equilibrium (i.e. constant voltage, load and motor speed) the equations of motion of a DC motor are:

$$V = RI + k_b\omega_{motor} \tag{7}$$

$$T_{motor} = k_t I - \nu\omega_{motor} \tag{8}$$

With R the motor resistance, k_t the motor's torque constant, k_b the motor's back emf constant, ν the motor's viscous friction constant, M the rotor's moment of inertia, ω_{motor} the rotor's angular velocity and T_{motor} the applied external load. The electric motor power is equal to the product of motor current and motor voltage. Assuming an instantaneous electric response for the transient behavior, the motor current and voltage can be calculated as a function of the motor acceleration, speed and load as follows:

$$I = \frac{M}{k_t}\dot{\omega}_{motor} + \frac{\nu}{k_t}\omega_{motor} + \frac{1}{k_t}T_{motor} \tag{9}$$

$$V = \frac{M\ R}{k_t}\dot{\omega}_{motor} + \frac{\nu\ R}{k_t}\omega_{motor} + k_b\,\omega_{motor} + \frac{R}{k_t}T_{motor} \tag{10}$$

Equations (9) and (10) will be used in section V to compared the modeled and measured electric motor power in Fig. 8.C.

V. Experimental results

In sections V-A and V-B, we aim to match the described SPEA model with motor torque and motor power measurements and as such validate the working principles of the SPEA. The required servomotor position is precalculated as a function of the required output position and torque via the model of section IV-B. The experiments are open-loop since only the servomotor position is PD-controlled and no damping control to avoid oscillations on the output is implemented. Therefore, the experiments in sections V-A and V-B are conducted at relatively low output speeds. In section V-C, however, the output angle ψ is kept constant and the output torque bandwidth of the SPEA PoC and the SEA are compared. In sections V-A, V-B and V-C the performed experiments and measurements are described. In section V-D the results of the experiments are discussed.

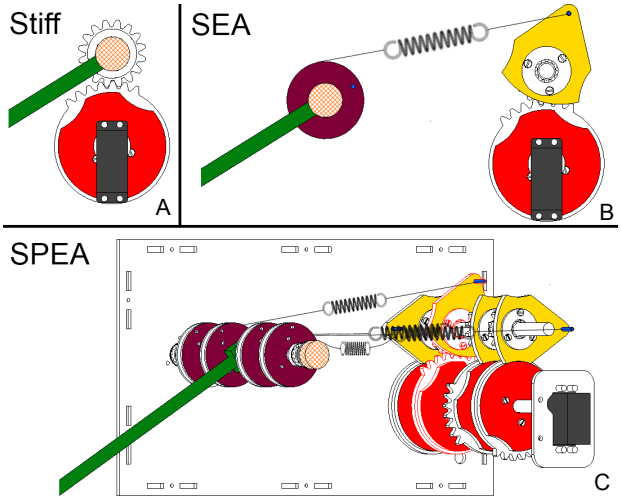

Fig. 6. The SPEA set-up with 4 springs in C, equivalent SEA in B and stiff set-up in A.

A. Motor torque measurements

The first experiment concerns three set-ups, namely, the SPEA set-up with 4 springs, the equivalent SEA ($k_{SEA} = 4k_{SPEA}$) and equivalent stiff set-up as shown in Fig. 6. The aim is to show the lowered motor torque for the SPEA, compared to the SEA and stiff actuator, while producing the same output torque. The output load (equal for all three set-ups) is a mass of 0.26 kg with its center of mass at 0.3 m from the output shaft. This load requires 0.77 Nm of output torque to statically hold the load at an output angle of $\psi = 90°$. The motor torque required to hold at each position between $\psi = 0°$ and $\psi = 90°$ is calculated for each of the three set-ups and shown in Fig. 7. Since the motor of both the SEA and stiff set-up in Fig. 6.B and A, is in series with the load, the maximum motor torque is almost the same for both set-ups as can be seen in Fig. 7. Both maxima are about twice the maximum output torque, which is $0.77\,Nm$, since the set-ups all have the extra $\epsilon = \frac{1}{2}$. The stiff curve goes from 0 Nm to the maximum torque in a sinusoidal way as expected. The SEA curve starts and ends at 0 Nm since the spring is locked in a singular position of no torque at the lever arm. The modeled SPEA motor torque is clearly lower than both serial set-ups. The modeled red dotted curve in Fig. 7 consists of 4 humps that logically resemble a scaled SEA curve since each of the 4 lever arms is locked in a singular position of no torque at the lever arm. The last hump is lower than the first hump due to the sagging of the springs.

In order to validate the modeled SPEA curve, the motor torque was measured approximately every time the output angle increased by $1°$ and plotted on top of the modeled curve. Each measurement is done at constant motor angle, which means the measured motor current I is directly related to the motor torque since $\omega_{motor} = 0$ in (8). Fig. 7 clearly shows that the measured SPEA motor torque follows approximately the model. The total torque produced by the pretensioned springs (yellow stripe dotted line in Fig. 7) rises and equals the total output torque when the output angle is at $90°$ and all springs

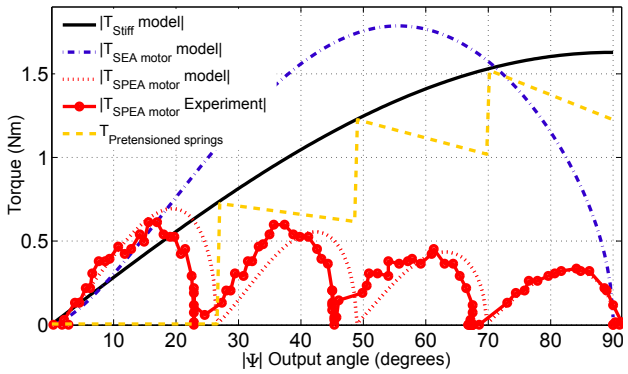

Fig. 7. The motor torque of the SPEA with 4 springs is clearly lower than the motor torque of the equivalent stiff and the SEA set-up. The measurements clearly match the modeled trend of reduced motor torque compared to the stiff and SEA set-ups.

are tensioned and locked.

B. Motor power measurements

The second experiment concerns three set-ups, namely, a SPEA set-up with 4 springs, a SPEA set-up with 2 springs and a stiff set-up. The aim is to show the decrease in electric motor power for a SPEA compared to the stiff set-up and to indicate the difference between a SPEA with 2 springs and a SPEA with 4 springs. The gravitational load is the same as for the torque measurements. Both the SPEAs (with 2 and 4 springs) need to track the same required output profile, namely the output profile of the stiff actuator (i.e. required output torque T_{req} and output velocity ω_{req}). The average measured output angle, out of 5 measurements, for the three set-ups is shown in Fig. 8.A. The three average curves are approximately the same. The standard deviation of each average curve is smaller than the linewidth and thus not plotted. The current and voltage of the motor in the three set-ups are measured and their product gives the measured electric motor power to deliver the output angle profile of Fig. 8.A. For each of the three set-ups the experiment is repeated 4 times and the average electric power of each set-up is plotted in Fig. 8.B. The standard deviation is plotted around the average curves with thin lines.

For the SPEA the equations (5) and (6) can be used to obtain the required motor torque and velocity based on the required output profile of Fig. 8.A. Next, the motor model of section IV-D enables to model the required motor electric power based on the required motor torques and velocities. The modeled electric motor power for the SPEA with 4 springs is plotted on top of the measurements in Fig. 8.C.

C. Output torque tracking

By means of this third experiment the output torque bandwidth of the SPEA PoC and the SEA (shown in Fig. 6.C and b) are compared. The SPEA and SEA are required to track a certain reference output torque trajectory while the output angle ψ is kept constant at 0°. The reference consists of 3 step responses with different maxima. The output torque is measured by means of a DRBK torque transducer with a measurement range of 20 Nm and a maximum combined

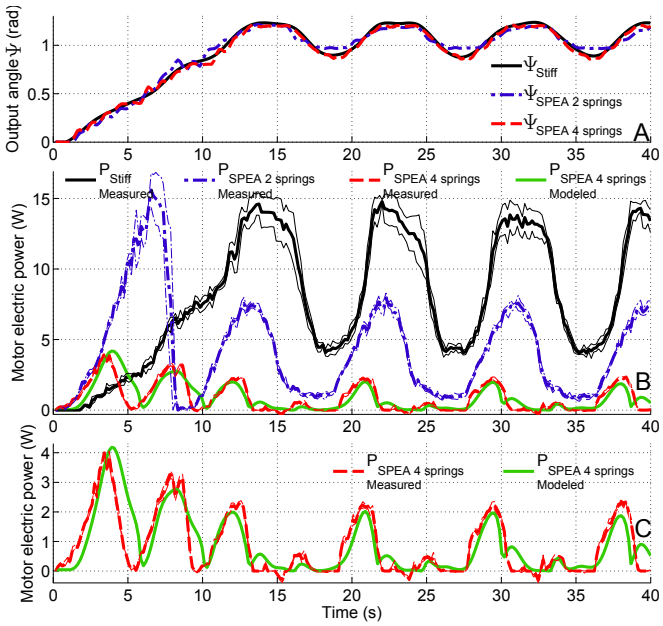

Fig. 8. A: The measured output angle for the three set-ups of the motor power experiment is comparable. B: The decrease in measured electric motor power as a function of parallel springs in the SPEA is clearly illustrated. C: The modeled electric motor power in a SPEA with four springs approximately matches the measurements.

error of 0.1 Nm. The control is open-loop since the required servomotor profiles are precalculated, based on the tracking reference, by means of the model described in section IV-A. In Fig. 9.A the measured output torque of the SEA (black solid line) and SPEA (red dashed line) are plotted and compared with the reference trajectory (black dotted line). Fig. 9.B, C, D and E shows the measured motor angle ϕ, motor voltage, motor current and motor electric power respectively. All data shown in Fig. 9 is averaged over 5 measurements. The standard deviation is plotted in thin lines around the measurements.

D. Discussion of results

The static motor torque experiment validates that the SPEA significantly lowers the motor torque compared to the equivalent stiff and SEA set-up. The maximum motor torque for the SPEA with 4 springs is not exactly 4 times lower as for the SEA with 1 spring but a bit higher. This is due to the sagging of the unpretensioned springs when output angle differs from 0°. The measured data clearly matches the model. Adding more springs in parallel in the SPEA will further decrease the motor torque, as indicated by (6) where an increase of n results in a reduction of T_{motor}.

Regarding the transient power measurements in Fig. 8.B, the conclusion follows that when more springs are used in parallel the power consumption decreases, while the mechanical power generated at the output link is for the different cases the same (since they track the same output profile as shown in Fig. 8.A). The integral of the three power curves in Fig. 8.B equals the energy required for each set-up: 320 J for the stiff set-up, 170 J for the SPEA with 2 springs and 34 J for the SPEA with 4 springs. This means the SPEA with 2 springs only requires 53% of the energy needed for the stiff set-up. For the

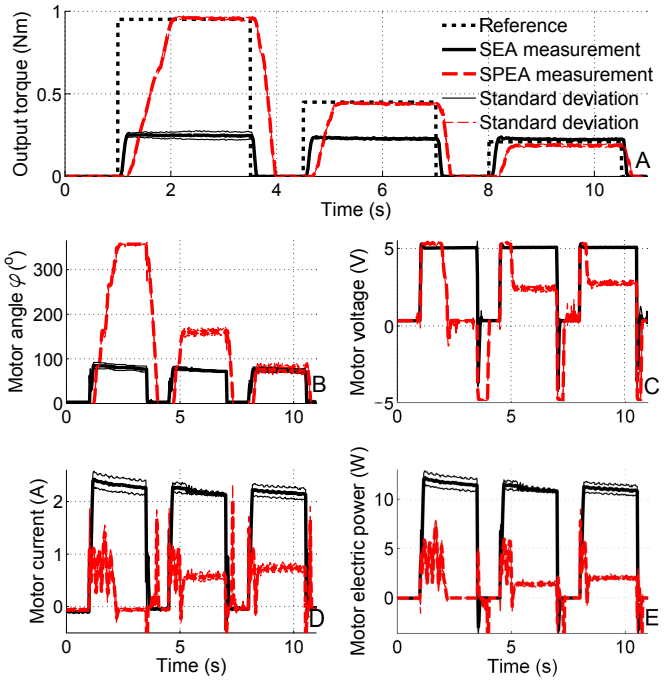

Fig. 9. Open loop output torque tracking experiments of the SPEA PoC and SEA with the output angle ψ constant at 0°. The measured output torque is given in A. The measured motor data is given in B,C,D and E.

SPEA with 4 springs this is only 11%. The main reason for this drastic increase in efficiency is the fact that the output torque $T_{SPEA} = T_{fix} + T_{variable}$, where T_{fix} is delivered by the locked springs and only $T_{variable}$ should be delivered by the motor. Since a lowered motor torque means a lowered current drain, the copper losses I^2R decrease as well. Fig. 8.C clearly shows that the modeled and measured power curves for the SPEA with 4 springs are approximately the same which validates our model.

Fig. 9.A shows that the SEA cannot deliver the reference output torque of the first 2 step responses while the SPEA can deliver all 3 step responses. In general, a SPEA with n springs in parallel can deliver approximately n times the maximum output torque of the SEA (for the PoC n=4). On the other hand, the motor angle in Fig. 9.B and step response rise time of the SPEA is approximately n times bigger compared to the SEA. It is important to note that the PoC results are determined by the maximum servomotor speed of 67 RPM. Fig. 9.E indicates that the SPEA electric motor power is lower than for the SEA. Moreover, when the output torque of the first step response is reached, the electric motor power equals 0 W due to the fact that all 4 springs are in pretensioned phase and no spring is in pretensioning phase. As such, all forces that are exerted to generate the output torque will not pass through the motor since it is not present in the force path. For the last two step responses, one spring remains in pretensioning phase and as such, the electric motor power is different from 0 W, though lower than the SEA.

VI. Conclusion and Future Work

In this paper, we introduced the novel SPEA compliant actuation concept based on an intermittent mechanism where parallel springs are tensioned and locked successively. The experiments showed that the SPEA concept can drastically lower the motor torque and energy requirements compared to a stiff actuator or a SEA, while maintaining the inherent compliance.

Currently mutilated gears are installed in the PoC as an intermittent mechanism. This can be further improved, since mutilated gears have some disadvantages such as the shocks at the transition between dwell and motion phases, the potential blocking of the mechanism and friction during the dwell phase. Moreover, the set-up currently only allows unidirectional torque output. We are investigating an improved intermittent mechanism which eliminates friction during the dwell phase, avoids potential blocking and shocks, and allows bidirectional torque output. Another interesting idea is to investigate, as was done for SEAs, the potential of variable stiffness in the SPEA.

Undiscussed so far is the increase in complexity and the potential increase in mass and volume of the SPEA as potential drawbacks, compared to stiff actuators and SEAs. We believe that these issues can be resolved since modern production techniques (such as 3D multi-material printing) are evolving at a speed which eliminates an increase in complexity as bottleneck. Furthermore, a SPEA with n springs will not necessarily weigh more than a SEA. There are indeed n dephased intermittent mechanisms, but these can be downgraded compared to the SEA mechanism since they are only subjected to a fraction of the total output torque. Furthermore, the motor and gearbox of the SPEA can be downgraded due to the reduced motor torque requirements, which means a reduction in size and weight as well, as calculated for the example of a transtibial prosthese in [18]. Future work consists in developing an optimization strategy for the SPEA design. Currently, the size and weight of the PoC are unoptimized.

Since a change of the output angle ψ of the SPEA tensions all parallel springs, the output behavior of the SPEA is identical to a SEA and the SPEA has practically the same overall output stiffness as an equivalent SEA. Therefore, the different control strategies developed for compliant actuators can also be used for the SPEA, for example to avoid oscillations by damping control, exploit natural dynamics for cyclic motions, etc., depending on the targeted application.

We hope that this novel actuation concept, which is biologically inspired by the variable recruitment of parallel muscle fibers, can contribute to the research towards more efficient actuators for the robots of tomorrow.

Acknowledgment

This work has been funded by the European Commission 7th Framework Program as part of the project H_2R (no.600698) and ERC-grant SPEAR (no.337596).

References

[1] G. A. Pratt and M. M. Williamson, “Series elastic actuators,” in *IEEE/RSJ International Conference on Intelligent Robots and Systems (IROS)*, vol. 1. IEEE, 1995, pp. 399–406.

[2] A. Bicchi, G. Tonietti, M. Bavaro, and M. Piccigallo, “Variable stiffness actuators for fast and safe motion control,” *International Journal of Robotics Research*, pp. 527–536, 2005.

[3] B. Vanderborght, N. G. Tsagarakis, R. Van Ham, I. Thorson, and D. G. Caldwell, "Maccepa 2.0: compliant actuator used for energy efficient hopping robot chobino1d," *Autonomous Robots*, vol. 31, no. 1, pp. 55–65, 2011.

[4] M. Laffranchi, N. Tsagarakis, and D. Caldwell, "Analysis and development of a semiactive damper for compliant actuation systems," *IEEE/ASME Transactions on Mechatronics*, vol. 18, no. 2, pp. 744–753, 2013.

[5] B. Vanderborght, A. Albu-Schaeffer, A. Bicchi, E. Burdet, D. Caldwell, R. Carloni, M. Catalano, O. Eiberger, W. Friedl, G. Ganesh *et al.*, "Variable impedance actuators: A review," *Robotics and Autonomous Systems*, vol. 61, no. 12, pp. 1601–1614, 2013.

[6] N. L. Tagliamonte, F. Sergi, D. Accoto, G. Carpino, and E. Guglielmelli, "Double actuation architectures for rendering variable impedance in compliant robots: A review," *Mechatronics*, vol. 22, no. 8, pp. 1187 – 1203, 2012.

[7] B. Vanderborght, B. Verrelst, R. Van Ham, M. Van Damme, P. Beyl, and D. Lefeber, "Development of a compliance controller to reduce energy consumption for bipedal robots," *Autonomous Robots*, vol. 24, no. 4, pp. 419–434, 2008.

[8] S. Davis, N. Tsagarakis, J. Canderle, and D. G. Caldwell, "Enhanced modelling and performance in braided pneumatic muscle actuators," *The International Journal of Robotic Research*, vol. 22, no. 22, pp. 213–227, 2003.

[9] R. Van Ham, B. Vanderborght, M. Van Damme, B. Verrelst, and D. Lefeber, "Maccepa, the mechanically adjustable compliance and controllable equilibrium position actuator: Design and implementation in a biped robot," *Robotics and Autonomous Systems*, vol. 55, no. 10, pp. 761–768, October 2007.

[10] J. W. Hurst and A. A. Rizzi, "Series compliance for robot actuation: Application on the electric cable differential leg," *IEEE Robotics & Automation Magazine*, vol. 15, no. 3, p. 2008, 2008.

[11] A. Jafari, N. Tsagarakis, B. Vanderborght, and D. Caldwell, "A novel actuator with adjustable stiffness (awas)," in *IEEE/RSJ International Conference on Intelligent Robots and Systems (IROS)*, 2010, pp. 4201–4206.

[12] A. Jafari, N. G. Tsagarakis, I. Sardellitti, and D. G. Caldwell, "A new actuator with adjustable stiffness based on a variable ratio lever mechanism," *IEEE/ASME Transactions on Mechatronics*, vol. PP, no. 99, pp. 1–9, jan 2013.

[13] S. Wolf, O. Eiberger, and G. Hirzinger, "The DLR FSJ: Energy based design of a variable stiffness joints," in *IEEE International Conference on Robotics and Automation (ICRA)*, 2011, pp. 5082–5089.

[14] R. Van Ham, T. Sugar, B. Vanderborght, K. Hollander, and D. Lefeber, "Review of actuators with passive adjustable compliance/controllable stiffness for robotic applications," *Robotics & Automation Magazine*, vol. 16, no. 3, pp. 81–94, 2009.

[15] (2012, Dec.) The mekabot website. [Online]. Available: http://mekabot.com/

[16] E. Guizzo and E. Ackerman, "The rise of the robot worker," *Spectrum, IEEE*, vol. 49, no. 10, pp. 34–410, October 2012.

[17] B. Vanderborght, A. Albu-schaeffer, A. Bicchi, E. Burdet, D. Caldwell, R. Carloni, M. Catalano, G. Ganesh, M. Garabini, G. Grioli, S. Haddadin, A. Jafari, M. Laffranchi, D. Lefeber, F. Petit, S. Stramigioli, M. Grebenstein, N. Tsagarakis, M. V. Damme, R. V. Ham, L. V. Visser, and S. Wolf, "Variable impedance actuators: Moving the robots of tomorrow," *IEEE/RSJ International Conference on Intelligent Robots and Systems (IROS Best jubilee video award)*, 2012.

[18] G. Mathijssen, P. Cherelle, D. Lefeber, and B. Vanderborght, "Concept of a series-parallel elastic actuator for a powered transtibial prosthesis," *Actuators*, vol. 2, no. 3, pp. 59–73, 2013.

[19] G. Pratt, "Challenges in actuation," in *IEEE International Conference on Robotics and Automation (ICRA) Workshop: Variable Stiffness Actuators moving the Robots of Tomorrow*, St. Paul - Minnesota, USA, May 2012.

[20] J. Madden, N. Vandesteeg, P. Anquetil, P. Madden, A. Takshi, R. Pytel, S. Lafontaine, P. Wieringa, and I. Hunter, "Artificial muscle technology: physical principles and naval prospects," *IEEE Journal of Oceanic Engineering*, vol. 29, no. 3, pp. 706 – 728, july 2004.

[21] B. Vanderborght, T. Sugar, R. Van Ham, K. Hollander, and D. Lefeber, "Comparison of mechanical design and energy consumption of adaptable passive compliant actuators," *International Journal of Robotics Research*, vol. 28, no. 1, pp. 90–103, January 2008.

[22] L. Visser, R. Carloni, and S. Stramigioli, "Energy-efficient variable stiffness actuators," *IEEE Transactions on Robotics*, vol. 27, no. 5, pp. 865 –875, October 2011.

[23] U. Mettin, P. X. La Hera, L. B. Freidovich, and A. S. Shiriaev, "Parallel elastic actuators as a control tool for preplanned trajectories of underactuated mechanical systems," *The international journal of robotics research*, vol. 29, no. 9, pp. 1186–1198, 2010.

[24] V. Arakelian and S. Ghazaryan, "Improvement of balancing accuracy of robotic systems: Application to leg orthosis for rehabilitation devices," *Mechanism and Machine Theory*, vol. 43, no. 5, pp. 565–575, 2008.

[25] J. Herder, "Design of spring force compensation systems," *Mechanism and machine theory*, vol. 33, no. 1, pp. 151–161, 1998.

[26] S. K. Au, J. Weber, and H. Herr, "Powered ankle–foot prosthesis improves walking metabolic economy," *IEEE Transactions on Robotics*, vol. 25, no. 1, pp. 51–66, 2009.

[27] D. F. B. Haeufle, M. D. Taylor, S. Schmitt, and H. Geyer, "A clutched parallel elastic actuator concept: Towards energy efficient powered legs in prosthetics and robotics," in *IEEE RAS EMBS International Conference on Biomedical Robotics and Biomechatronics (BioRob)*, 2012, pp. 1614–1619.

[28] J. Bickford, *Mechanisms for intermittent motion*. Industrial Press New York, 1972.

[29] N. Sclater, *Mechanisms and mechanical devices sourcebook*. McGraw-Hill Professional, 2011.

[30] E. Burdet, R. Osu, D. Franklin, T. Milner, and M. Kawato, "The cns skillfully stabilizes unstable dynamics by learning optimal impedance," *Nature*, vol. 414, pp. 446–449, 2001.

[31] R. M. Alexander, *Exploring Biomechanics: Animals in Motion*. Scientific American Library, 1992.

[32] A. Hill, *First and last experiments in muscle mechanics*. University Press Cambridge, 1970.

[33] E. Henneman, "Relation between size of neurons and their susceptibility to discharge," *Science*, vol. 126, no. 3287, pp. 1345–1347, 1957.

Glenn Mathijssen was born in 1989. He received the degree in study of Mechanical Engineering at the Vrije Universiteit Brussel (VUB) in 2012. He is PhD researcher at the Robotics and Multibody Mechanics research group. His research includes compliant actuation, energy-efficient actuation and humanoids (European FP7-project H_2R and ERC-grant SPEAR).

Dirk Lefeber obtained a PhD in Applied Sciences at the Vrije Universiteit Brussel, in 1986. He is head of the Robotics and Multibody Mechanics Research Group. From 2000 to 2004 and from 2008 till 2012 he was head of the department of Mechanical Engineering. He is a member of IEEE and CLAWAR. He is author/co-author of 4 books, three book chapters, 27 journal papers and about 60 international conference papers over the past five years. He is involved in multiple national and European projects.

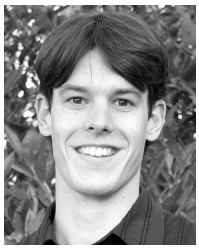

Bram Vanderborght obtained a PhD in Applied Sciences in 2007. In 2006 he performed research on the humanoids robot HRP-2 at JRL in AIST, Tsukuba (Japan). From 2007-2010 he worked as post-doc researcher at the Italian Institute of Technology in Genua on the humanoid robot iCub and compliant actuation. Since 2009 he is appointed as professor at the VUB. He is a member of IEEE. His research includes cognitive and physical human robot interaction, robot assisted therapy, compliant actuation, humanoids and rehabilitation robotics. He is involved in multiple national and European projects, and the ERC-grant SPEAR.